ISSN 1070-3632, Russian Journal of General Chemistry, 2015, Vol. 85, No. 5, pp. 1167–1173. © Pleiades Publishing, Ltd., 2015.

Selective Synthesis of Copper Microsheets and Ultralong Microwires via a Surfactant Assisted Hydrothermal Process[1]

S. Dehghanpour[a], A. Mahmoudi[b], and S. Shadpour[b]

[a] *Department of Chemistry, Alzahra University, P.O. Box 1993891176, Tehran, Iran*
e-mail: dehghanpours@alzahra.ac.ir
[b] *Department of Chemistry, Islamic Azad University, Karaj Branch, Karaj, Iran*

Received December 31, 2014

Abstract—The surfactant assisted hydrothermal process for selective preparation of copper nanosheets and ultralong microwires by reducing Cu^{2+} with 2-(bis-phosphonomethylamino)propionic acid (dpc) under the action of cetyltrimethylammonium bromide (CTAB) or polyvinyl pyrrolidine (PVP) is presented. X-ray powder diffraction (XRD) and energy dispersive X-ray analysis (EDX) indicate that the products are pure Cu of cubic phase. The effects of starting material concentration and reaction time on morphology of nanosheets have been studied by scanning electron microscopy (SEM). The presence of CTAB and PVP as capping agents is identified by EDX, transmission electron microscopy (TEM) and FT-IR. The possible growth process for ultralong microwires was studied by stopping the growth at a series of intermediate morphology stages based on SEM observations. Optical properties of Cu nanosheets and ultralong microwires were studied by UV–Vis spectrophotometry.

DOI: 10.1134/S107036321505028X

INTRODUCTION

Inorganic materials of all dimensions, from nano to microscale, have been intensively studied due to their size and shape dependent optical, electrical and magnetic properties [1–3]. Among metals Cu nano/micro structures have attracted considerable attention due to their potential applications in thermal conductivity, lubrication, and as catalysts [4–6]. Up to now, copper nano/micro structures with different shapes have been prepared by a number of synthetic methods, including polyol process, templated synthesis, reverse micelles, microemulsion, electrochemical deposition, chemical process in solutions, chemical vapor deposition, and irradiation [7–14]. Previously we had succeeded in making a full range of novel three dimensional copper microstructures by a complex precursor hydrothermal route in highly basic media using diphosphonocarboxylate ligand as the complexing agent and reducer [15].

In the present study we have focused on preparation of one and two dimensional copper microstructures given their promising applications in electronic, optoelectronic and magnetic devices [16, 17]. Low dimensional growth can be achieved by using a static template, which enhances the growth rate of one crystallographic face over another. For example, Sun and co-workers [18] have synthesized Cu nanoplates and nanowires by reducing Cu^{+} with ascorbic acid in presence of CTAB or CTAC. Qian and co-authors [13] have presented complex surfactant assisted hydrothermal reduction approach to synthesis of copper nanowires in presence of sodium dodecylbenzenesulfonate (SDBS).

In this study facile reduction hydrothermal method that involved various surfactants made it possible to identify two different morphologies of copper nanosheets and microwires. Cu nanosheets synthesis was supported by CTAB and microwires were obtained under the action of PVP. Concentration of starting materials and reaction time influenced upon morphology of synthesized microstructures. The products were characterized by XRD, EDX, SEM, TEM, FT-IR, and UV–Vis spectrophotometry.

RESULTS AND DISCUSSION

Copper nanosheets were synthesized in presence of dpc via the simple surfactant assisted hydrothermal

[1] The text was submitted by the authors in English.

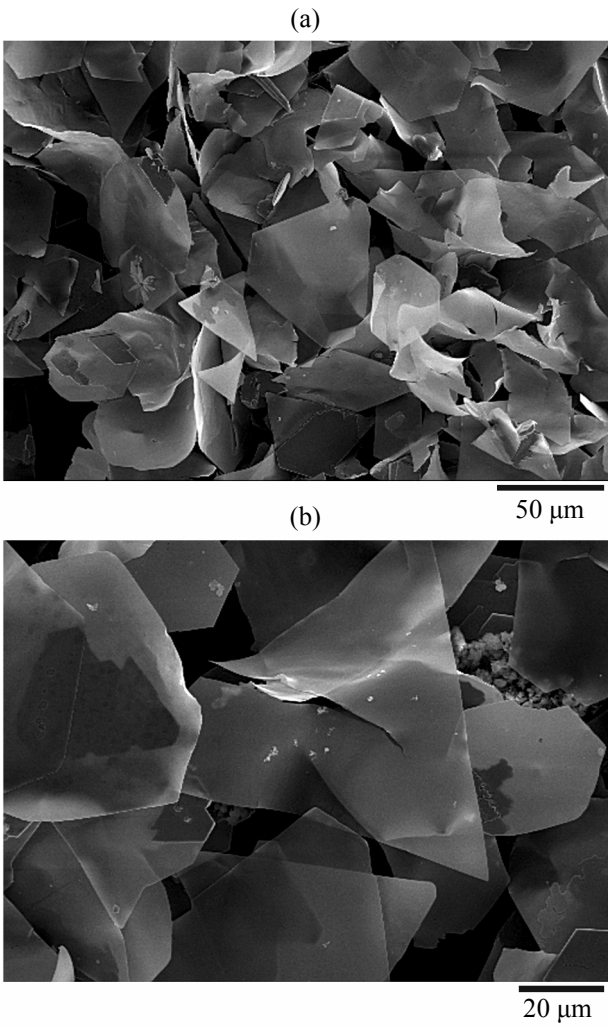

Fig. 1. (a) Low and (b) high magnification SEM images of copper nanosheets synthesized with CTAB (0.23 mmol) for 4 h. The inset of Fig. 1b shows a magnified view of the edge of a nanosheet.

route. It is well known that diphosphonocarboxylate derivatives had been widely used for synthesis of inorganic organic hybrid materials [19, 20]. Therefore, formation of copper nanosheets involved at least two steps including Cu^{2+}-diphosphonocarboxylate complex formation by reaction of $Cu(CH_3COO)_2{\cdot}2H_2O$ with dpc ligand in aqueous solutions. Formation of the complex was confirmed by IR spectra, ν, cm^{-1}: 1195–919 (s, M–OP, $–PO_3$); 3500–3000 (s), 1695–1633 (w, coordinated water); 2850–2650 (P–OH); 2350–2100 (P–O–H); 2991, 2918 (s, CH_2.); 1457 (d, CH_2); 1684 (C=O) [19, 20]. Composition of all synthesized compounds was also supported by elemental analysis. Upon formation of Cu^{2+}-diphosphonocarboxylate complex the carboxylic acid group of dpc ligand reduced

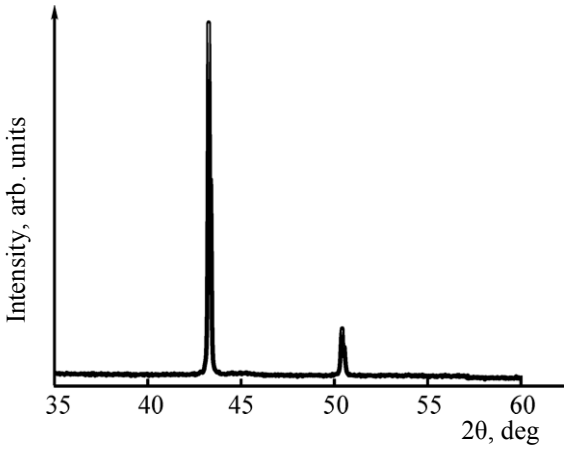

Fig. 2. XRD pattern of copper nanosheets synthesized with CTAB (0.23 mmol) for 4 h.

Cu^{2+} to Cu^0 particles [21–23] and then the suitable concentration of CTAB provided favorable conditions for growth of anisotropic nanosheet structures.

Low and high magnification SEM images demonstrated that the products were nanosheets with lateral dimension of up to 50 μm (Figs. 1a, 1b). Most nanosheets had hexagonal, triangular and truncated triangular shapes. High magnification SEM images (Fig. 1b) indicated that thickness of copper nanosheets was in the range of ca 150–250 nm. The nanosheets had transparent surface with the same thickness even at the edges.

All XRD peaks (Fig. 2) could be indexed to the (111) and (200) planes of the face centered cubic (fcc) structure of Cu (space group $Pn3m$; a_0 = 3.615 Å; JCPDS card no. 4-836). No peaks of impurities were detected. The intensity ratio of the (111) diffraction peak, up to 200, in XRD patterns was higher than the reference value [15], which implied that the basal planes of the nanosheets were dominated by {111} facets and therefore their {111} planes had prevailing parallel orientation to the surface of the substrate.

Strong EDX peaks (Fig. 3) were attributed to copper. Peaks assigned to O and C indicated presence of the capping agent. Cu nanosheet solutions were extremely stable over weeks of storage with no evidence of oxidation of the particles. Significant stabilization of the particles presumably was due to surface capping of Cu nanosheets by CTAB molecules.

Presence of a capping agent on the surface of Cu nanosheets had also been confirmed by FT-IR (Fig. 4, curves *1* and *2*). The C–H symmetric and asymmetric

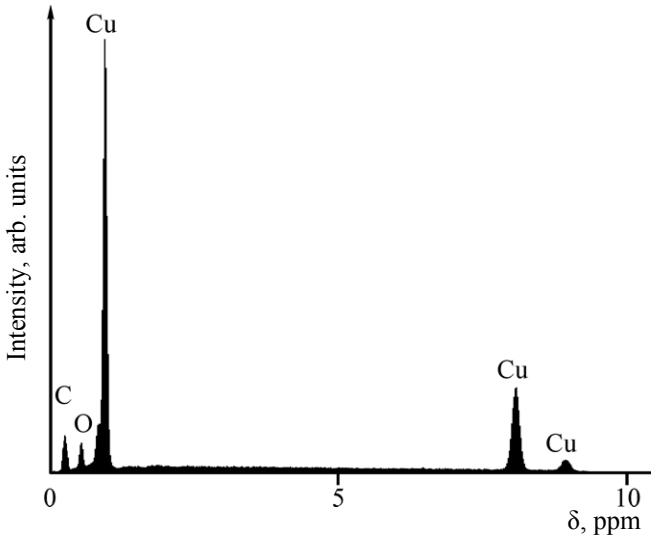

Fig. 3. EDX analysis of copper nanosheets synthesized with CTAB (0.23 mmol) for 4 h.

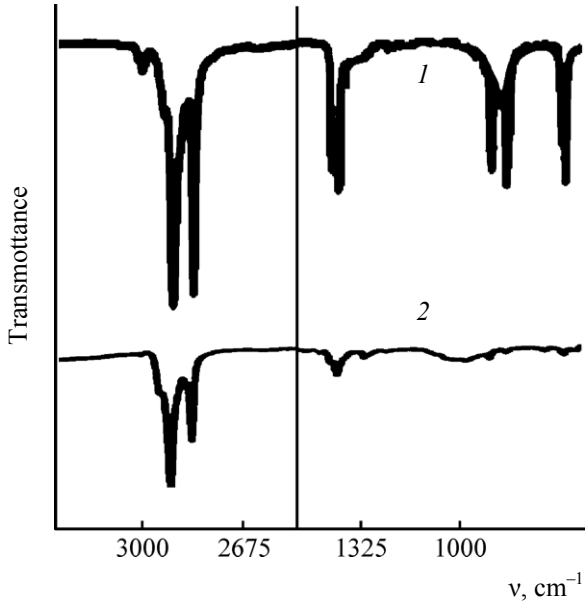

Fig. 4. FT-IR spectra of pure (*1*) CTAB and (*2*) CTAB-capped Cu nanosheets.

stretching vibration of CH_2 groups (2954, 2917, and 2850 cm^{-1}) were recorded for pure CTAB (curve *1*). The bands at 1472 and 1462 cm^{-1} (curve *2*) were attributed to the CH_2 scissoring mode of vibration. Copper nanosheets bands at 2924, 2854, 1474 and 1464 cm^{-1} (curve *2*) assigned to C–H stretching and C–H bending, respectively [24–26] indicated presence of CTAB on the surface of copper nanosheets.

Clear surface structures of the single copper nanosheets demonstrated by TEM could not be shown because of the large scale. Therefore, only part of the structure is shown in TEM image (Fig. 5). Light and dark contrast is clearly observed along the radial direction. The dark contrast indicates Cu crystals with larger mass thickness in the core region. Outside the core region the light contrast suggests that the layer is the capping agent.

Longer reaction time (8 h) resulted in formation of samples consisting of flexural nanosheets with thickness of about 400–600 nm and an average diameter ranging from 60 to 100 micrometers (Fig. 6a). Most of nanosheets demonstrated truncated corners or curves at the edges.

The above experimental data indicated that Cu nanosheets could be synthesized via a simple hydrothermal method. However, it is well known that sheet like structures in the face centered cubic metal are of higher energy than the thermodynamically favored shapes (truncated cubes) [18]. With the appropriate reduction rate, kinetic control dominates in both nucleation and growth of Cu particles. In our system, with dpc used as the reducing agent, release rate of free Cu^{2+} was controlled by the newly formed Cu^{2+}-diphosphonocarboxylate complex. In such case the controlled release of Cu^{2+} ions modified the reduction process, which might affect the competition between kinetic and thermodynamic factors during reduction of precursors, nucleation, and growth of Cu

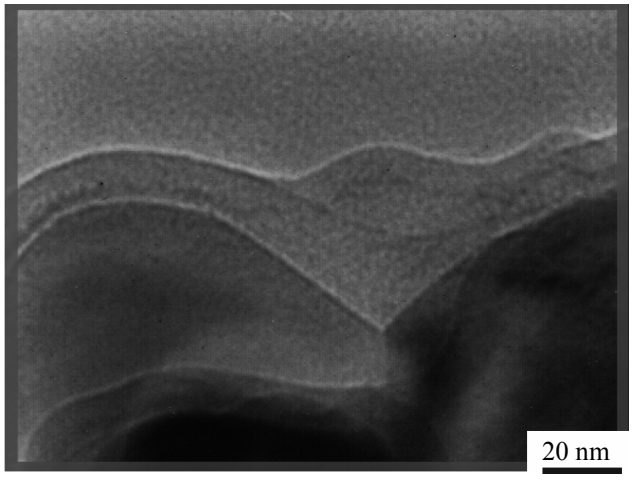

Fig. 5. TEM image of a fragment of Cu nanosheet synthesized with CTAB (0.23 mmol) for 4 h.

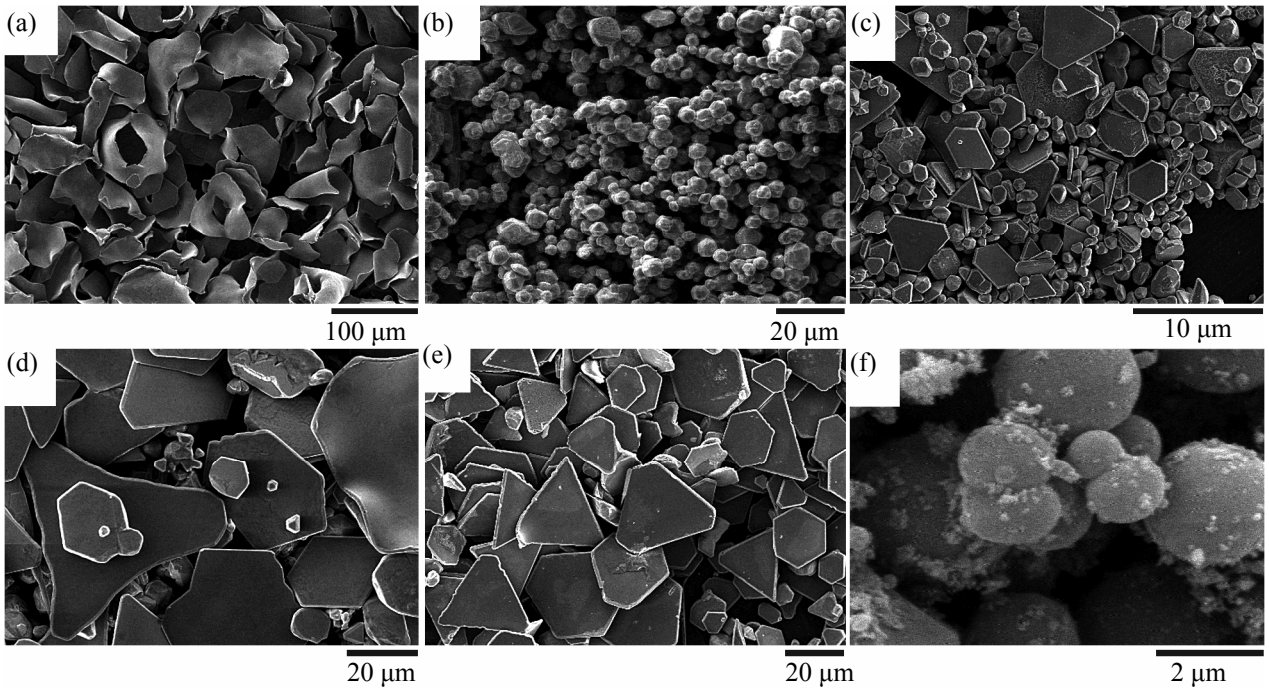

Fig. 6. SEM images of Cu nanosheets synthesized with (a) CTAB (0.23 mmol) for 8 h, (b) CTAB (0.23 mmol) and alanine (0.23 mmol) instead of dpc. for 4 h, (c) CTAB (0.23 mmol) and dpc (0.23 mmol) for 4 h, (d) CTAB (0.8 mmol) for 4 h, (e) CTAB (1.5 mmol) for 4 h, and (f) CTAB (8 mmol) for 4 h.

crystals. The proper Cu^{2+} concentration may provide favorable conditions for growth of anisotropic sheet like structures in presence of CTAB. When dpc was substituted by alanine release rate of Cu^{2+} from Cu $(CH_3COO)_2{\cdot}2H_2O$ was in favor of formation of the irregular copper particles (Fig. 6b). When the concentration of dpc was low (0.23 mmol), Cu $(CH_3COO)_2{\cdot}2H_2O$ could not transform into Cu^{2+}-diphosphonocarboxylate complex completely. Under such conditions the release rate of Cu^{2+} was controlled by both $Cu(CH_3COO)_2{\cdot}2H_2O$ and Cu^{2+}-diphosphonocarboxylates complexes irregular particles and nanosheets coexisting in the products.

Concentration of CTAB influenced upon size and shape of Cu microcrystals. CTAB could possibly control the kinetic factors of growth rates of different crystalline faces by interacting with those faces via poisoning mechanism. The poison adsorbed on some crystalline faces could decrease the growth rates and lead to highly anisotropic growth [18].

The effect of CTAB concentration on morphology of Cu structure was studied experimentally while keeping the other conditions constant. The triangular or hexagonal shaped sheets of Cu in case of the basal plane {111}, the side plane or edge of the sheet should be bound by {100} plane [27]. At low concentration of CTAB in the reaction solution Cu atoms tended to assemble around copper nuclei forming large particles that had a tendency to adsorb CTAB on the {111} planes, hence, reducing the growth rate of those faces. As a result {100} plane adsorbed fewer CTAB molecules and grew quicker than {111} faces that could be favorable for growth of copper nanosheets. At higher CTAB concentration adsorption of CTAB on {100} and {111} planes increased leading to inhibition of the anisotropic growth of sheets. Microsheets with thickness ca 1 μm and diameter ca 20–60 μm were obtained when the amount of CTAB was increased to 0.8 mmol (Fig. 6d). Higher amount of CTAB (1.5 mmol) led to copper microsheets (Fig. 6e) with thickness ca 1.5 μm and an average diameter ranging from 10 to 30 μm. A complete coverage of surface of copper particles (8 mmol) by CTAB favored an isotropic growth for all faces resulting in formation of microspheres (Fig. 6f).

It has been widely reported that the shape of metals nano and micro structures could be controlled by the type of a surfactant [10]. Addition of PVP instead of CTAB in the process media ultralong copper microwires were formed. Phase type and purity of the

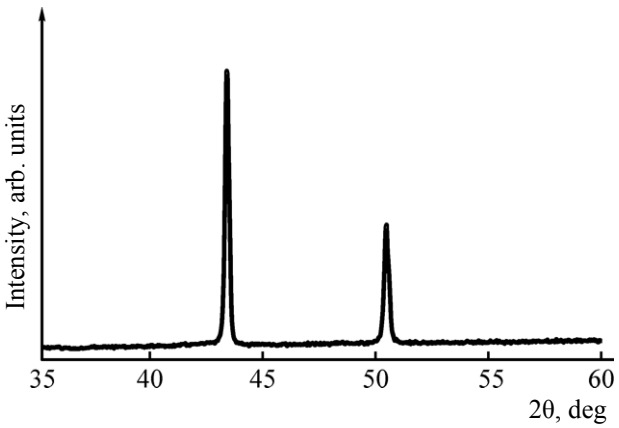

Fig. 7. XRD pattern of ultralong copper microwires formed after 4 h.

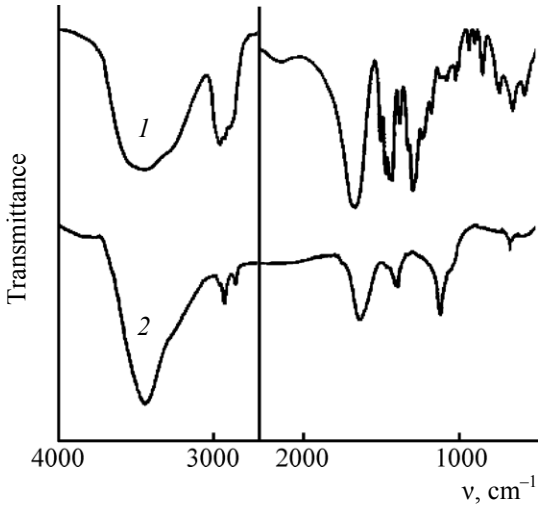

Fig. 8. FT-IR spectra of (*1*) pure PVP and (*2*) PVP-capped Cu microwieres.

products were confirmed by the XRD pattern (Fig. 7). All peaks could be indexed as FCC Cu with lattice constant a = 3.615 Å which was very close to the reported earlier values (space group $Pn3m$; JCPDS card no. 4-836). In the X-ray pattern no characteristic peaks corresponding to impurities of oxides were detected even upon weeks of storage which could be due to presence of PVP as a capping agent on the surface of copper microwires. The same was also confirmed by IR spectra (Fig. 8). The bands at 1020 and 1075 cm^{-1} of pure PVP correspond to the C–N bending modes and were strengthened and shifted to 1035 and 1077 cm^{-1}, respectively, in Cu microwires spectrum. The shift of the C–N band indicated chemical coordination of nitrogen atoms to Cu microwires surface [28]. The band of C=O at 1645 cm^{-1} of pure PVP became narrower and shifted to 1635 cm^{-1} in the spectrum of Cu microwires. Red shift of PVP C=O frequency for 20 cm^{-1} indicated formation of >C=O–Cu bonds [28]. The band provided evidence for incorporation of PVP into Cu microwires. SEM images of products (Figs. 9a–9c) indicated formation of large quantity of ultralong copper microwires with the diameter of 2–3 μm and length ca 850–950 μm, thus featuring an aspect ratio ca 300.

Time dependent growth of ultralong copper microwires was carried out upon hydrothermal treatment for 0.5, 2.0 and 4.0 h (Figs. 10a–10c)**.** Besides copper microlance, Cu microparticles could be observed, suggesting that copper microlance was formed by aglomeration of microparticles in the course of heating process. SEM images (inset in Fig. 10a) revealed that some of the microparticles were decahedrons. Upon

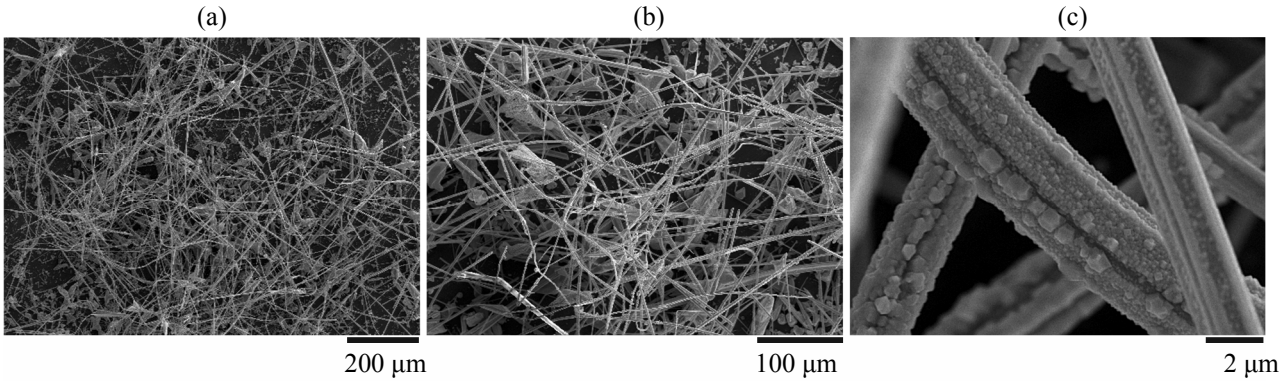

Fig. 9. (a) Low and (b) high magnification SEM images of ultralong Cu microwires formed after 4 h, (c) typical ultralong Cu microwires.

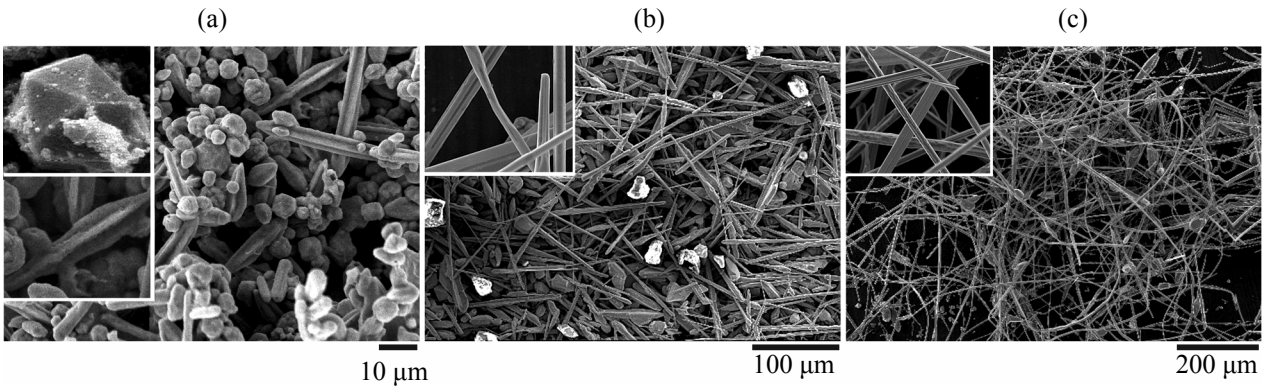

Fig. 10. SEM images of ultralong Cu microwires during the shape evolution: (a) 0.5 h, (b) 2 h and (c) 4 h.

aging for 2 h the product was composed of microwires with length of 80–150 μm along with irregular aggregates (Fig. 10b). Heating of the mixture for 4 h led to ultralong microwires with uniform diameter (Fig. 10c) in accordance to the Ostwald ripening process [29]. The growth mode was similar to the recently reported one for FCC nanorods and nanowires [30]. For instance, copper nanowires with controllable aspect ratio were prepared by using poly(allylamine) (PAAm) as the capping reagent [30]. In another example, silver nanorods and nanowires are grown with PVP as the capping reagent, whose oxygen atoms bind most strongly to the {100} facets of Ag [28]. Those structures evolved from multiple twinned 10 facets particles (MTPs). Anisotropic growth of decahedral seeds could facilitate formation of a 1D structure (Scheme 1). Presence of a capping agent could change the order of free energies for various crystallographic planes and thus their relative growth rates. In our study PVP acted the similar way transforming decahedral MTPs of copper into ultralong Cu microwires.

In UV–Vis spectra Cu nanosheets were characterized by the band at 610 nm and ultralong microwires demonstrated absorption at 650 nm [13, 18] indicating that optical properties of new Cu structures were dependent on morphology of the products.

In summary, Cu nanosheets and ultralong Cu microwires have been selectively synthesized via surfactant assisted hydrothermal process. Cu nanosheets were synthesized upon the action of CTAB surfactant. The experiments confirmed that the release rate of Cu^{2+} in the system and concentration of CTAB play critical roles in controlling morphology of Cu nanosheets. Application of PVP surfactant instead of CTAB resulted in formation of ultralong microwire structures. In the course of shape evolution of ultralong Cu microwires, according to SEM data, a series of structures with intermediate morphologies were formed making it possible to speculate on probable reaction mechanism.

Scheme 1. Schematic illustration of the mechanism proposed for growth of a nanowire with pentagonal cross sections from a decahedral seed.

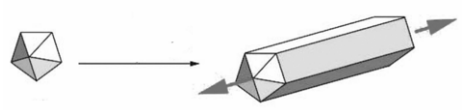

EXPERIMENTAL

Reagent grade chemicals were obtained from commercial sources and used without further purification. Deionized water was used in the experiments. 2-(Bis-phosphonomethyl-amino)-propionic acid and $HOOCCH(CH_3)N(CH_2PO_3H_2)_2$, (dpc) were prepared according to the Moedritzer-Irani synthesis [31, 32]. SEM images were obtained on a Philips XL-30ESEM equipped with an X-ray energy dispersive detector. TEM images were obtained on a PHILIPS CM120. XRD patterns of samples were recorded on a PHILIPS PW 1800 X-ray powder diffractometer with CuK_α (λ = 1.5406 Å) radiation. FT-IR spectra (KBr discs) were recorded using a NICOLET IR 100 Spectrophotometer. UV-Vis spectra were recorded on a JASCO V-570 spectrophotometer. Elemental analyses for the synthesized Cu^{2+}-diphosphonocarboxylate hybrid. Found, %: C 16.14, H 4.07 and N 3.81%. $Cu(C_5H_{11}NO_8P_2\cdot(H_2O)_2$. Calculated, %: C 16.03, H 4.04 and N 3.74.

General procedure for Cu nanosheets and ultralong Cu microwieres. *a*. Synthesis of Cu^{2+}-diphosphonocarboxylates complex-precursors: To a solution of $Cu(CH_3COO)_2\cdot H_2O$ (46 mg, 0.23 mmol) in 10 mL

of distilled water was added dpc (63.7 mg, 0.23 mmol). The mixture was stirred at room temperature for 40 min.

b. Formation of Cu nanosheets and ultralong Cu microwieres: Upon stirring the above mixture for 40 min CTAB (0.84 mg) was added. After 5 min of vigorous stirring the mixture was placed into a Teflon-lined autoclave (23 mL capacity) and maintained there at 170°C for 4 h, then cooled down to room temperature. Thereafter, the dispersions were purified by centrifugation redispersion cycles with each successive supernatant being decanted and replaced with ethanol. Finally the product was dried in a vacuum oven. When CTAB was substituted by PVP (K-30) (50 mg) the reaction procedure and conditions remained the same.

ACKNOWLEDGMENTS

This worl wasfinancial support by Alzahra University is gratefully acknowledged.

REFERENCES

1. Sun, S.H., Murray, C.B., Weller, D., Folks, L., and Moser, A., *Science*, 2000, vol. 287, p. 1989.
2. Millstone, J.E., Park, S., Shuford, K.L., Qin, L., Schatz, G.C., and Mirkin, C.A., *J. Am. Chem. Soc*., 2005, vol. 127, no. 15, p. 5312.
3. Nam, J.M., Thaxton, C.S., and Mirkin, C.A., *Science*, 2003, vol. 301, no. 5641, p. 1884.
4. Choi, H. and Park, S. H., *J. Am. Chem. Soc*., 2004, vol. 126, no. 20, p. 6248.
5. Kim, C., Gu, W.H., Briceno, M., Robertson, I.M., Choi, H., and Kim, K., *Adv. Mater*., 2008, vol. 20, no. 10, p. 1859.
6. Liu, Z. and Bando, Y., *Adv. Mater*., 2003, vol. 15, no. 4, p. 303.
7. Qi, L., Ma, J., and Shen, J., *J. Colloid Interface Sci*., 1997, vol. 186, no. 2, p. 498.
8. Lisiecki, I., Biorling, M., Motte, L., Ninham, B., and Pileni, M.P., *Langmuir*, 1995, vol. 11, no. 7, p. 2385.
9. Zhao, Y., Zhu, J.J., Hong, J.M., Bian, N., and Chen, H.Y., *Eur. J. Inorg. Chem*., 2004, vol. 2004, no. 20, p. 4072.
10. Becerril, H.A., Stoltenberg, B.M., Monson, C.F., and Woolley, A.T., *J. Mater. Chem*., 2004, vol. 14, p. 611.
11. Shin, H.C., Dong, J., and Liu, M., *Adv. Mater*., 2003, vol. 15, no. 19, p. 1610.
12. Zhang, M., Lenhert, S., Wang, M., Chi, L., Lu, N., Fuchs, H., and Ming, N., *Adv. Mater*., 2004, vol. 16, no. 5, p. 409.
13. Liu, Z., Yang, Y., Liang, J., Hu, Z., Li, S., Peng, S., and Qian, Y., *J. Phys. Chem. B*, 2003, vol. 107, no. 46, p. 12658.
14. Kapoor, S., Palit, D.K., and Mukherjee, T., *Chem. Phys. Lett*., 2002, vol. 355, no. 3-4, p. 383.
15. Dehghanpour, S., Mahmoudi, A., Mirsaeed-Ghazi, M., Bazvand, N., Shadpour, S., and Nemati, A., *Powder Technol*., 2013, vol. 246, p. 148.
16. Hu, J., Odom, T.W., and Lieber, C.M., *Acc. Chem. Res*., 1999, vol. 32, no. 5, p. 435.
17. Tian, Z., Voigt, J., Liu, J., Mckenzie, B., Mcdermott, M.J., Rodriguez, M.A., Konishi, H., and Xu, H., *Nat. Mater*., 2003, vol. 2, p. 821.
18. Xu, S., Sun, X., Ye, H., You, T., Son, X., and Sun, S., *Mater. Chem, Phys*., 2010, vol. 120, no. 1, p. 1.
19. Chandrasekhar, V., Azhakar, R., Senapati, T., Thilagar, P., Ghosh, S., Verma, S., Boomishankar, R., Steiner, A., and Koegerler, P., *Dalton Trans*., 2008, no. 9, p. 1150.
20. Cabeza, A., Aranda, M.A.G., and Bruque, S., *J. Mater. Chem*., 1999, vol. 9, no. 2, p. 571.
21. Yan, Y., Wu, C.D., and Lu, C.Z., *Z. Anorg. Allg. Chem*., 2003, vol. 629, no. 11, 1991.
22. Zhang, X.M., *Coord. Chem. Rev*., 2005, vol. 249, nos. 11–12, p. 1201.
23. Chen, X.M. and Tong, M.L., *Acc. Chem. Res*., 2007, vol. 40, no. 2, p. 162.
24. Saterlie, M.S., Sahin, H., Kavlicoglu, B., Liu, Y., and Graeve, O.A., *Chem. Mater*., 2012, vol. 24, no. 12, p. 3299.
25. Kung, K.H.S. and Hayes, K.F., *Langmuir*, 1993, vol. 9, no. 1, p. 263.
26. Bellamy, L.J., *The Infrared Spectra of Complex Molecules*, New York: Chapman & Hall, 1975.
27. Chen, S. and Carroll, D.L., *J. Phys. Chem. B*, 2004, vol. 108, no. 18, p. 5500.
28. Borodko, Y., Habas, S.E., Koebel, M., Yang, P., Frei, H., and Somorjai, G.A., *J. Phys. Chem. B*, 2006, vol. 110, no. 46, p. 23052.
29. Sun, Y., Mayers, B., Herricks, T., and Xia, Y., *Nano Lett.*, 2003, vol. 3, no. 7, p. 955.
30. Wang, Y. and Asefa T., *Langmuir*, 2010, vol. 26, no. 10, p. 7469.
31. Moedritzer, K. and Irani, R.R., *J. Org. Chem*., 1966, vol. 31, no. 5, p. 1603.
32. Dehghanpour, S., Mahmoudi, A., Esbati, F., and Hadian-rasanani, S., *Mater. Res. Bull*., 2012, vol. 47, p. 2126.